# Komaiitic Chlorite-amphibole Rocks and Mafic Metavolcanics from the Karasjok Greenstone Belt, Finnmark, Northern Norway: A Preliminary Report

HELGE HENRIKSEN

Henriksen, H. 1983: Komatiitic chlorite-amphibole rocks and mafic metavolcanics from the Karasjok greenstone belt, Finnmark, northern Norway: a preliminary report. *Norges geol. Unders. 382,* 17–43.

A general account is presented of the field relationships, geochemistry and petrology of mafic and ultramafic metavolcanics within the Precambrian Karasjok greenstone belt. These metavolcanic rocks make up the major part of this greenstone belt, and are variably deformed and metamorphosed in middle greenschist to lower amphibolite facies. Based on their unusual chemistry (21–39% MgO volatile-free) and extrusive textures, the ultramafic chlorite-amphibole rocks are considered to belong to the komatiite association. The mafic metavolcanics (amphibolites) form a tholeiitic series (5–8% MgO volatile-free), and are chemically similar to intermediate and iron-rich tholeiites of Archaean age. The mutual occurrence of these komatiitic and tholeiitic series as well as the presence of exhalative-sedimentary Fe-Mn formations in association with the komatiites, would suggest that the Karasjok greenstone belt forms an extension of the 2.6–2.75 Ga Archaean greenstone belts of eastern and northern Finland.

*Helge Henriksen, A/S Sydvaranger prospektering, postboks 83, 1321 Stabekk, Norway*

## Introduction

The Precambrian basement in the Karasjok area of northern Norway (Fig. 1) is made up of four, main, N–S trending, geological units (from west to east): (a) a granite-gneiss complex, (b) the Karasjok greenstone belt, (c) a belt with dominantly hornblende gneisses and (d) a granulite complex.

*The granite-gneiss complex* consists of several generations of granitic rocks. Polyphasally-deformed homogeneous to banded gneisses of granodioritic to tonalitic compositions appear to be the oldest components of the granite-gneiss complex. These polyphasally-deformed rocks are intruded by tonalitic rocks of more massive appearance. Potassic granites represent a third generation of granitic rocks in the granite-gneiss complex. Little is known about the structural and metamorphic history of this complex, and few radiometric ages are available. Samples from SE of Skoganvarre (Fig. 1) have yielded Archaean (2800 Ma.) U–Pb zircon ages (Merilainen 1976).

A *metasedimentary formation* (the *Skoganvarre formation)* forms a narrow band along the eastern margin of the granite-gneiss complex. This formation is claimed to rest with a primary unconformity upon the granite-gneiss complex. (e.g. near Skoganvarre, see Skålvoll 1972). Recent mapping by the author has shown, however, that in other places the interface between the granite-gneiss complex and the Skoganvarre formation is strongly tectonized and folded.

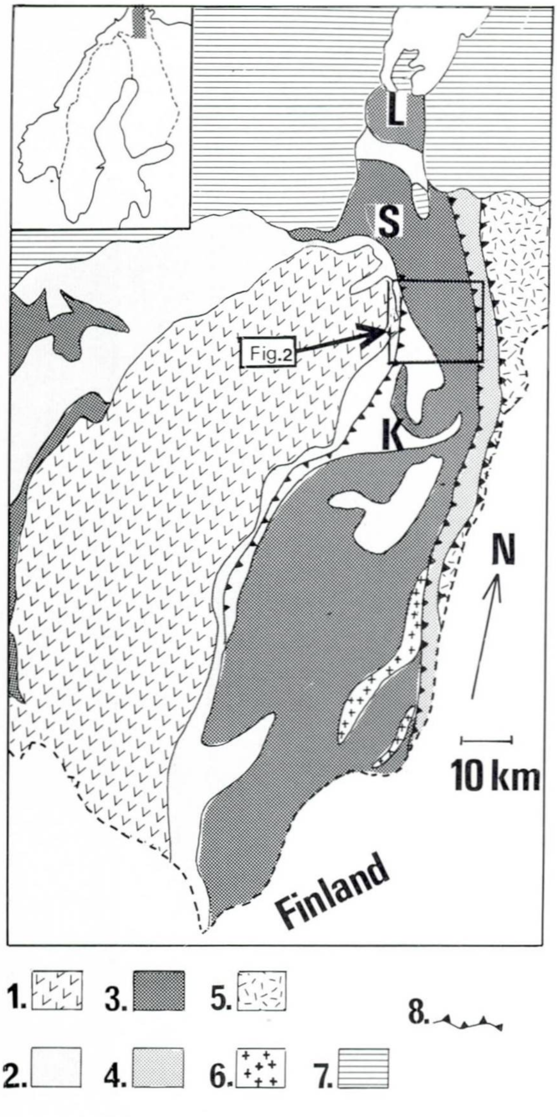


*Fig. 1.* Simplified geological map of the Karasjok district, based on Wennervirta (1969) and Skålvoll (1972) and unpublished work by Henriksen (1980, 1982).
1. Granite–gneiss complex, 2. Metasedimentary formations in the K.G.B., 3. Metavolcanic formations in the K.G.B., 4. Hornblende gneisses, 5. Granulite Complex, 6. Microcline granites, 7. Palaeozoic nappes and post-Archaean formations, 8. Tectonic/thrust contacts. K – Karasjok, L – Lakselv, S – Skoganvarre.

The Skoganvarre formation commences in places with conglomerates that contain large, angular clasts of granitic rocks (U-Pb zircon age 2800 Ma., Skålvoll 1972), passing up into arkosic grits and psammitic lithologies. Towards the top of the succession, quartzitic metasediments and/or fuchsite-carbonate rocks occur in alternation with metaconglomerates.

Although original clastic grains are preserved in coarser-grained, gritty lithologies, the influence of penetrative deformations and metamorphic recrystallization is clearly seen in the rocks of the Skoganvarre formation. Mineral assemblages in psammitic-pelitic lithologies reflect metamorphic recrystallization in the middle greenschist facies (biotite grade).

The rocks of the *Karasjok greenstone belt* (K.G.B.) show thrust contacts against both the granite-gneiss complex and the Skoganvarre formation. The K.G.B. is dominated by mafic and ultramafic metavolcanics, which together with gabbroic rocks form the largest portion of the greenstone belt. The metasedimentary rocks are of a varied nature including calcareous biotite schists, phyllites, quartz-sericite schists, psammitic and arkosic metasediments, quartzites and graphitic schists. Smaller metamorphosed ultrabasic, tonalitic and granitic intrusives are also present. The metamorphic grade in the K.G.B. varies from the middle greenschist facies (biotite grade) in the western parts to low amphibolite facies in the easternmost parts.

The K.G.B. has traditionally been assigned a Proterozoic age (e.g. Skålvoll 1972, Bugge 1980). However, Meriläinen (1976) obtained a zircon age of about 2720 ma. from an albite-diabase in the K.G.B., and work in progress by the author shows that there are strong lithological and chemical similarities between the K.G.B. and the 2.75–2.6 Ga. old greenstone belts in northern Finland (e.g. Gaal et al. 1978).

East of the K.G.B., banded *hornblende gneisses* of tholeiitic geochemical affinities extend along the west side of the arcuate granulite zone (Fig. 1). These rocks appear to form a separate geological unit of volcanic-sedimentary origin (Meriläinen 1976, Barbey et al. 1980, Henriksen 1980, 1982, Hörmann et al. 1980). Few radiometric ages are available from this unit, but an Archaean age has been assumed by Meriläinen (1976), Barbey et al. (1980) and Hörmann et al. (1980). Thrust contacts occur between the K.G.B. and the hornblende gneisses, and between the hornblende gneisses and the granulite complex.

The quartzo-feldspathic gneisses of the *granulite complex* are considered by Barbey et al. (1980) to represent a thick sedimentary prism of continental provenance. Radiometric ages range from 2600 Ma. (total rock lead) to 1836 Ma. (Rb–Sr), and an Archaean age is generally accepted for this complex (e.g. Simonen 1980). According to Meriläinen (1976) the rocks of the granulite complex were metamorphosed for the first time in the amphibolite facies about 2500 Ma. ago. It is further claimed by Meriläinen (1976) and Simonen (1980) that these rocks were metamorphosed in the granulite facies during the Proterozoic (about 2150 Ma.ago), and later overthrust towards the southwest under conditions of granulite to high-amphibolite facies about 1900 Ma. ago. This view is at variance with that of Råheim and Bugge (in prep.), who consider the tectono-metamorphic evolution of the granulite complex in terms of an Archaean (2500–2600 Ma.) high-grade granulite event and a superimposed low/medium grade Svekokarelian (1850 ± 75 Ma) deformational/metamorphic event which has resulted, in places, in strong retrogression.

## Main features of the Karasjok greenstone belt

### STRATIGRAPHY AND ROCK TYPES

Scarce and isolated outcrops and a polyphasal deformational history make it difficult to decipher the original stratigraphic relations in the K.G.B. A metasedimentary succession of interbanded graphitic biotite schists, phyllites, psammites and fuchsite-bearing quartzites, which contain minor intercalations of mafic and ultramafic metavolcanics, is considered to represent the lowermost stratigraphic level in the sedimentary-volcanic pile. This dominantly sedimentary unit is followed by a thick unit of mafic and ultramafic metavolcanics (amphibolites and chlorite-amphibole rocks), interbanded with minor quartzitic and pelitic metasediments. This volcanic unit is in turn succeeded by arkosic and quartzitic metasediments which contain minor pelitic horizons.

Meta-ultrabasites and metagabbroic rocks occur as conformable lenses with tectonized margins in the supracrustal sequence. Although primary minerals and textures may be present, deformation and metamorphic recrystallization has resulted in the production of a variety of secondary assemblages. In the meta-ultrabasites, assemblages of antigorite + chlorite ± talc ± tremolite ± carbonate are the most common. Assemblages of hornblende and saussuritized plagioclase are the most frequent in the gabbroic rocks. The supracrustal sequence is also intruded by hornblende-bearing tonalitic rocks. Variably deformed and recrystallized potassic granites, possibly of several generations, are also present.

The relationships between the volcanic-sedimentary pile and the shallow-water metasedimentary rocks of the Skoganvarre formation is presently under investigation. Although the K.G.B. has been thrust against the Skoganvarre formation, its present tectonic position does not necessarily imply the involvement of large lateral translations. There is no clear metamorphic break between the two units, and their different lithological character could reflect a lateral lithological variation within the same sedimentary-volcanic basin. The presence of fuchsite-bearing sedimentary rocks in both units is interesting, as these rocks *may* coincide with the onset of the ultramafic volcanicity in the K.G.B. Other potential source rocks for the Cr-rich metasediments of the Skoganvarre formation are, as yet, not known. The possibility that at least the upper parts of the Skoganvarre formation were deposited at a late stage in the development of the K.G.B. thus cannot be ruled out.

To summarize, the relationships at Skoganvarre suggest an interpretation of the granite-gneiss complex as the basement, and the Skoganvarre formation as a sedimentary cover sequence which shows a lateral transition into the K.G.B. per se. On the other hand, only very limited work has been carried out in the gneiss area, which makes it difficult to relate any structural events in *these* rocks to the sequence of structural events in the K.G.B. One puzzling feature is the apparent lack of clasts showing unambiguous pre-conglomerate deformational fabrics in the conglomeratic sediments of the Skoganvarre formation. Hence, the assertion that the granite-gneisses did not have a pre-greenstone belt structural history, but were deformed and metamorphosed for their first time together with the sedimentary-volcanic rocks of the greenstone belt, cannot be excluded.

## SUMMARY OF STRUCTURAL AND METAMORPHIC EVENTS

The earliest phase of deformation recognized in the K.G.B. ($D_1$) caused a transposition of the primary layering in the sedimentary rocks into the limbs of isoclinal $F_1$ folds with northerly axial trends. The metamorphism ($M_1$) synchronous with $D_1$ resulted in the formation of a penetrative planar fabric ($S_1$), commonly a schistosity or compositional banding. This composite foliation is the dominant planar fabric within the K.G.B., and strikes NNW–SSE with moderate dips towards the northeast. Although no conclusive evidence has been found, certain features in a few outcrops may suggest that $S_1$ was the result of more than one deformation. The $M_1$ metamorphism, which extended into the post-tectonic stage, produced mineral assemblages varying from the middle greenschist facies (biotite grade) in the western parts of the K.G.B. to lower amphibolite facies in the easternmost parts.

During the second phase of deformation ($D_2$), $S_1$ was folded by tight to isoclinal, reclined folds with easterly plunges and northeasterly-dipping axial surfaces. Easterly-plunging lineations are commonly associated with the hinge regions of the $F_2$ folds. Shear-zones and smaller thrust faults along the limbs of the overturned $F_2$ folds were also developed during this stage. The main planar fabric ($S_2$) produced during $M_2$ was a differentiated crenulation cleavage transitional to a schistosity in micaceous lithologies, and a blastomylonitic foliation in thrust- and shear-zones. The $S_1$ and $S_2$ planar fabrics are in general parallel (except in the hinges of $F_2$ folds), reflecting the strong re-orientation of the pre-$D_2$ structures during $D_2$. The metamorphism ($M_2$) which accompanied $D_2$ was clearly retrograde and replaced such $M_1$ minerals as garnet and staurolite with secondary assemblages of chlorite and sericite.

During a late stage of $D_2$ the rocks of the K.G.B. were brought into tectonic contact with the Skoganvarre formation and the granite-gneiss complex. The thrusting of the K.G.B. was associated with the formation of low-grade, $S_2$-foliated blastomylonitic rocks. Similar low-grade blastomylonitic rocks are found between the K.G.B. and the hornblende gneisses in the east and appear also to be present between the hornblende gneisses and the granulite complex. All of these zones may have formed as a response to the final thrusting of the granulite complex during the Proterozoic (cf. Bugge 1960).

The latest deformation recorded in the K.G.B. was that responsible for the formation of NE- and SE-trending faults and crush-zones.

## The Ultramafic Chlorite-Amphibole Rocks

In the southern part of the K.G.B. at Njuovcokka, Wennervirta (1969) recognized ultramafic chlorite-amphibole rocks which contained volcanic (agglomeratic) structures. Recent geological mapping by the author has led to the discovery of similar ultramafic metavolcanics in an area to the north of Karasjok, and it is clear that these rocks are ubiquitous members of the volcanic-sedimentary pile of the K.G.B. The chlorite-amphibole rocks occur mainly as conformable bands or isolated hinges of $F_1$ folds in the mafic-ultramafic volcanic unit, but are also present as intercalations in the lower metasedimentary unit (Fig. 2).

Whole-rock and selected trace-element analyses from the chlorite-amphibole rocks is presented in Table 1 together with reference analyses from the literature. Table 1 demonstrates the chemical similarities of the ultramafic chlorite-amphibole rocks from Karasjok and the high-magnesium komatiite suite of Archaean greenstone belts.

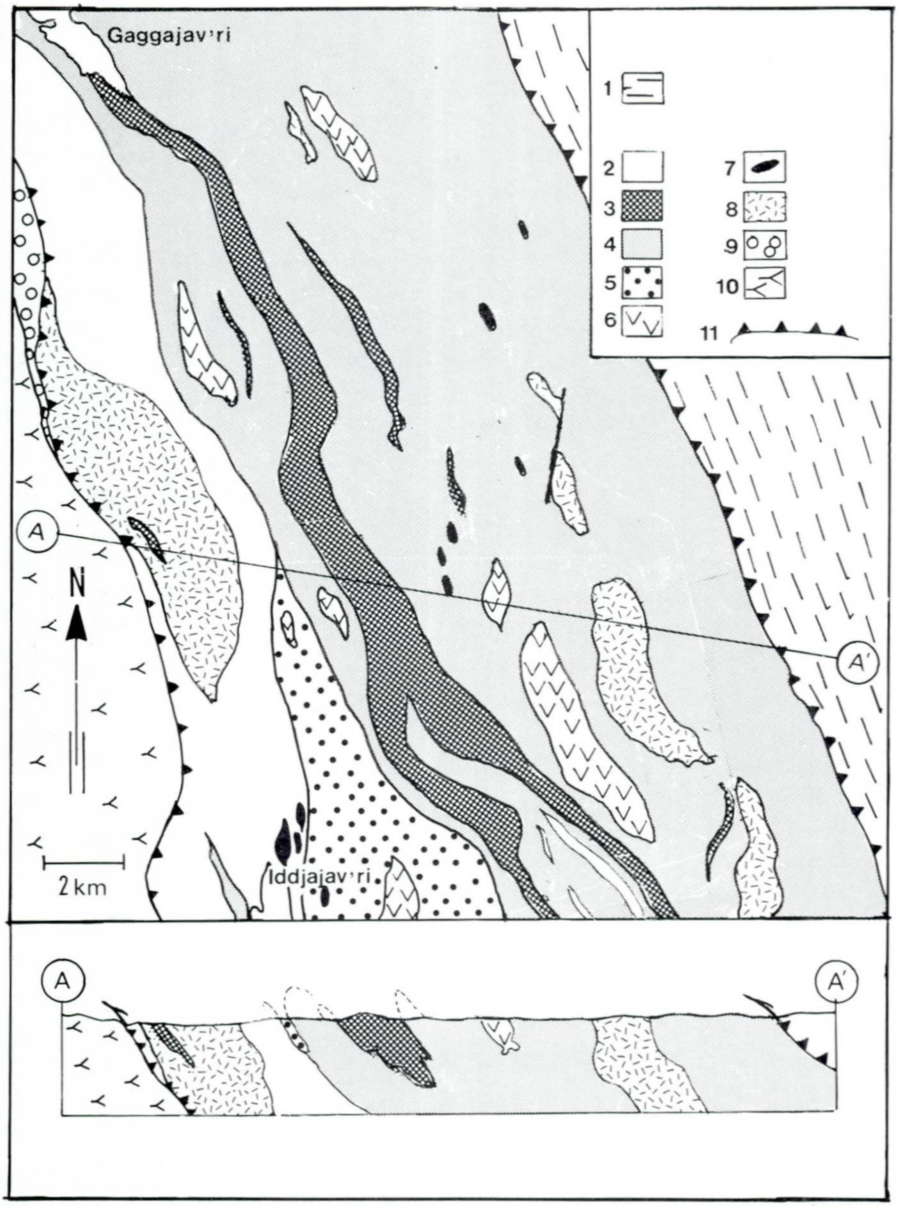


*Fig. 2.* Simplified geological map with cross-section of a part of the Karasjok greenstone belt north of Karasjok. Key: 1. Hornblende gneisses, 2. Metasediments (interbanded biotite schists, phyllites, psammites and fuchsite-bearing quartzites), 3. Chlorite-amphibole rocks, 4. Amphibolites, 5. Arkosic metasediments, 6. Metagabbro, 7. Meta-ultrabasites, 8. Tonalitic and granodioritic rocks, 9. Skoganvarre formation, 10. Granite gneiss, 11. Tectonic/thrust contacts.

The term komatiite was first used by Viljoen & Viljoen (1969) for an unusual series of ultrabasic and basic lavas in the Barberton greenstone belt having high MgO (>9%), Ni and Cr contents, low $TiO_2$ (<1%) and alkali contents, and with characteristically high $CaO/Al_2O_3$ ratios ($\geqq 1$). Another characteristic feature of these rocks is the presence of spinifex textures, indicating their formation from crystal-free, high-magnesian liquids.

A variety of classifications, based on both chemical and textural criteria, has later been proposed for such high-magnesian volcanic rocks (e.g. Brooks & Hart 1974, Arndt et al. 1977, Nisbet et al. 1977, Arndt et al. 1979). For a review, the reader is referred to Condie (1981). Arndt et al. (1977) suggested a wider definition of komatiite and introduced the term 'komatiite series' for a wide range of noncumulate and cumulate rocks ranging from peridotitic to andesitic compositions. It was believed that all members of the komatiite series could be derived by crystal fractionation and accumulation from a primary silicate liquid whose composition was represented by that of the spinifex-textured periodotitic ($MgO > 20\%$) members.

The Penrose conference on komatiites (see Arndt & Brooks 1980) proposed that the term komatiite should not refer to a member of a rock suite, but to a rock type like basalt or andesite. The conference thus defined komatiite as an ultramafic volcanic rock with $MgO \geqq 18\%$. Arndt & Nisbet (1982) suggested redefining komatiite as an ultramafic volcanic rock, i.e. a lava or volcanoclastic rock with $> 18\%$ MgO. It was also suggested that komatiites form the ultramafic portion of the komatiitic magmatic suite, which also include genetically related mafic volcanics called komatiitic basalts.

Based on their field appearance and textures, the chlorite-amphibole rocks from Karasjok can be identified as either volcanic or cumulate rocks. An assessment of Table 1 shows that they satisfy the general chemical criteria listed for komatiites. Their chemical composition in terms of MgO and their volcanic textures classify these rocks as komatiites according to the definitions of Arndt & Brooks (1980) and Arndt & Nisbet (1982).

## METAVOLCANIC CHLORITE–AMPHIBOLE ROCKS

The metavolcanic chlorite-amphibole rocks have a characteristic greenish-grey colour. Depending on the degree of deformation, they are either massive chlorite-amphibole rocks or well foliated chlorite-amphibole schists. Evidence of their extrusive nature is preserved where the rocks are least deformed, and include such primary volcanic features as pillows and polyhedral joints.

The pillowed units (about 10 m thick) display unambiguous pillow structures. The pillows show a wide range in size and shapes. Most commonly, they are balloon-like to oval in shape, with long axes from 20 to 70 cm in length. Near the top of one pillowed unit, large tube-like pillows, budding-pillows and branching pillows (cf. Vuagnat 1975) have been observed. Individual pillows may be polyhedrally jointed, or have radial joints (Fig. 3). Siliceous sedimentary material may locally occupy the interstices between adjacent pillows.

Polyhedral joints are present in otherwise massive chlorite-amphibole rocks. They divide the rock into angular polyhedra ranging from a few cm to 30 cm across (Fig. 4). A structure similar to polyhedral jointing is composed of angular fragments with pale-coloured rims, and may represent fractured flow tops.

Some authors (e.g. Nisbet et al. 1977, Condie 1981) have suggested that the

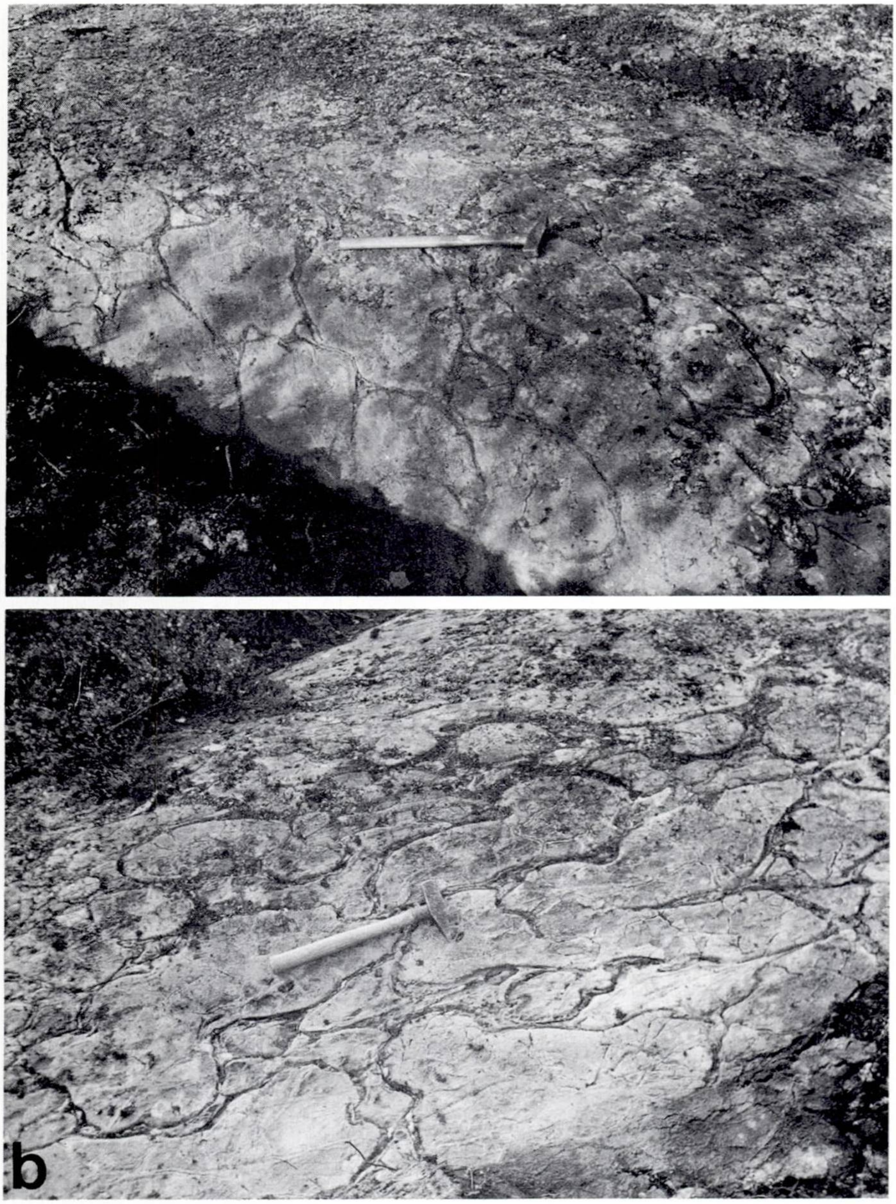


*Fig. 3.* Pillow structures from the ultramafic metavolcanics: (a) pillow lava composed of ultramafic chlorite-tremolite rocks (analyses 14–15); (b) branching and budding pillow forms in chlorite-amphibole rocks. Individual pillows show polyhedral jointing.

term komatiite should be restricted to ultramafic lavas exhibiting spinifex textures. The spinifex texture, which is thought to form by rapid crystal growth from low viscosity, Mg-rich melts, is characterized by a random or parallel orientation of elongate olivine and/or clinopyroxene. The olivine spinifex texture is considered by many authors as a prime characteristic and a diagnostic feature of peridotitic

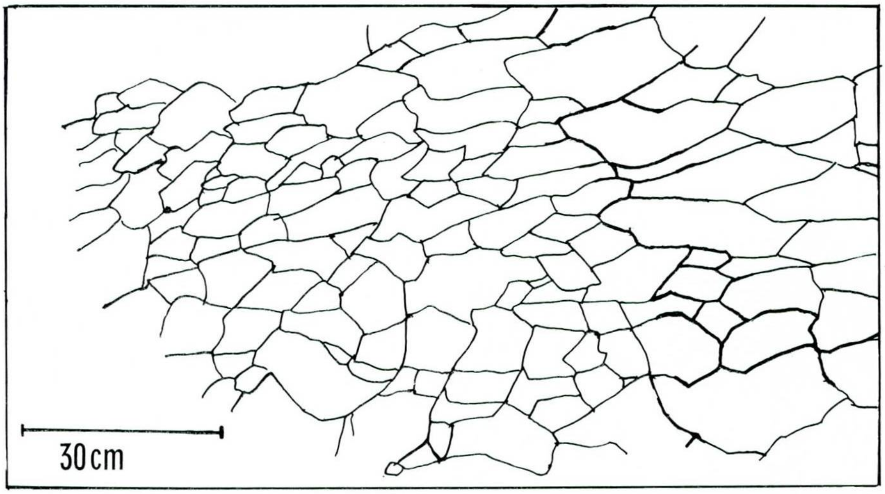


*Fig. 4.* Polyhedrally jointed surface of otherwise massive chlorite-amphibole rock. Drawn from a photograph.

komatiites (Nesbitt et al. 1979, Condie 1981). However, according to Arndt et al. (1979), the absence of spinifex texture does not necessarily mean that a rock is not komatiitic. In many Archaean areas spinifex-textured lavas form either very small portions of otherwise massive flows, or grade along strike into massive flows devoid of the spinifex texture.

In the rocks from Karasjok, identification of spinifex textures is made difficult by the combined effects of metamorphism and deformation. On the regional scale, the metamorphism is dynamic, and associated with the production of penetrative schistosities which have obliterated most primary features. The common mineral assemblage recorded from the metavolcanic chlorite-amphibole rocks

*Mg-chlorite + tremolite ± antigorite ± carbonate ± olivine*

is entirely metamorphic and consistent with prograde metamorphic recrystallization of a primary ultramafic assemblage under conditions ranging from upper greenschist facies to low amphibolite facies (Evans & Frost 1975). A typical example of the recrystallized chlorite-amphibole rocks is shown in Fig. 5a. This metamorphic fabric is in places overgrown by colourless porphyroblasts of olivine.

There are, however, domains in competent ultramafic lithologies which have escaped pervasive deformation and where the metamorphism has been essentially static. These domains are characterized by the lack of a schistosity, and retain primary volcanic structures even though the mineral assemblages are secondary. A review of the literature (Binns et al. 1976, Arndt et al. 1977, Willet et al. 1978) shows that the net result of prograde metamorphism of spinifex-textured ultramafic komatiites under such conditions is the replacement of the primary phases by a variety of secondary hydrous minerals. Olivine is pseudomorphed by platy Mg-chlorite or antigorite, and the original glass is replaced by submicroscopic intergrowths of chlorite and serpentine. In areas of low strain, spinifex textures may be excellently preserved, even though the alteration is complete.

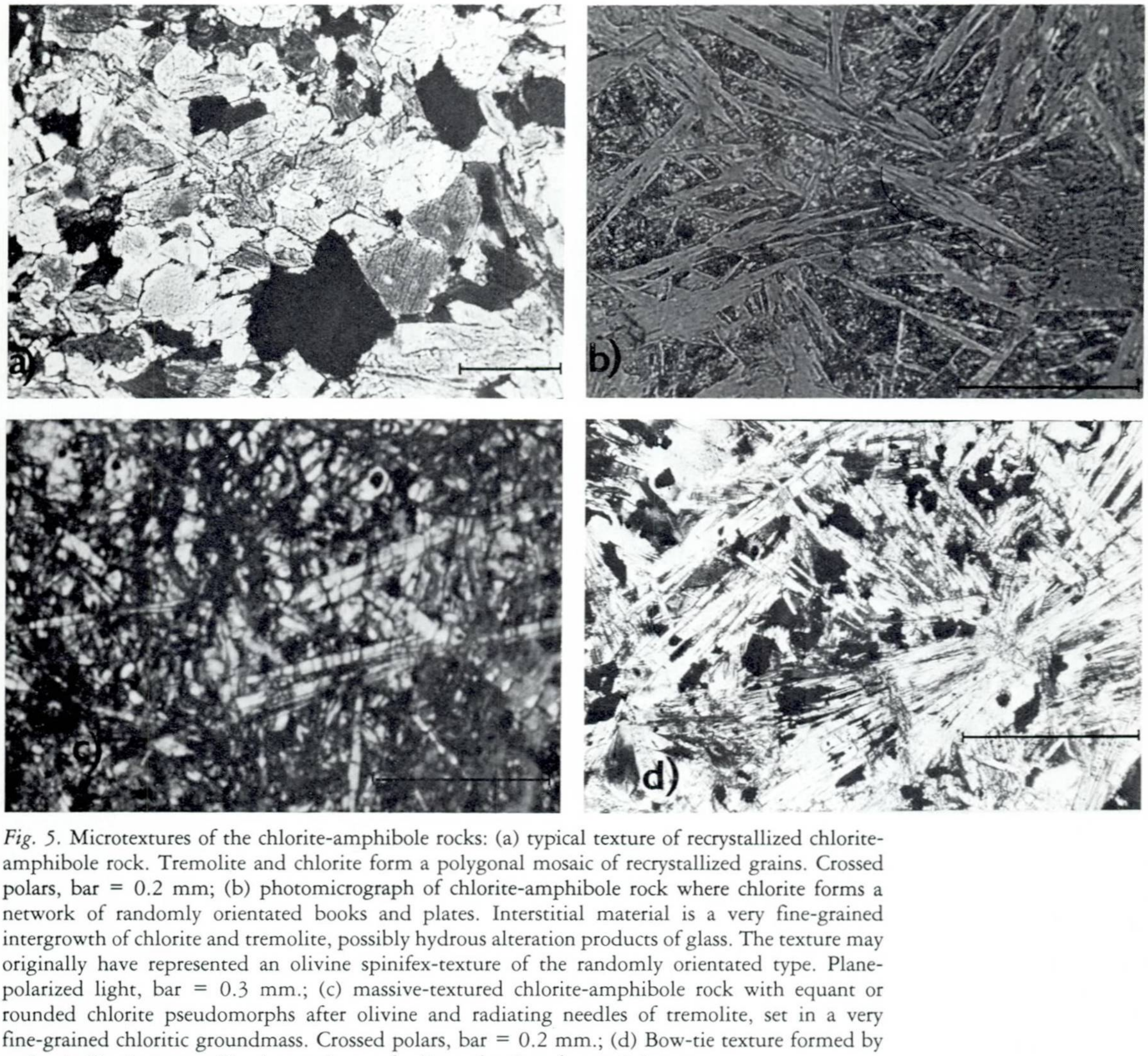


*Fig. 5.* Microtextures of the chlorite-amphibole rocks: (a) typical texture of recrystallized chlorite-amphibole rock. Tremolite and chlorite form a polygonal mosaic of recrystallized grains. Crossed polars, bar = 0.2 mm; (b) photomicrograph of chlorite-amphibole rock where chlorite forms a network of randomly orientated books and plates. Interstitial material is a very fine-grained intergrowth of chlorite and tremolite, possibly hydrous alteration products of glass. The texture may originally have represented an olivine spinifex-texture of the randomly orientated type. Plane-polarized light, bar = 0.3 mm.; (c) massive-textured chlorite-amphibole rock with equant or rounded chlorite pseudomorphs after olivine and radiating needles of tremolite, set in a very fine-grained chloritic groundmass. Crossed polars, bar = 0.2 mm.; (d) Bow-tie texture formed by anthophyllite in recrystallized cumulate rock. Crossed polars, bar = 0.9 mm.

The textural features exhibited by the last deformed chlorite-amphibole rocks from Karasjok are shown in Fig. 5b. The texture is dominated by randomly orientated books of Mg-chlorite and antigorite. They are set in a very fine grained groundmass that consists mainly of felty intergrowths of chlorite, which may represent altered glass. This texture displayed by the chlorite-amphibole rocks closely resembles the texture of spinifex-textured komatiitic rocks which have been metamorphosed in the upper greenschist/low amphibolite facies (cf. Willet et al. 1978), and presumably represents pseudomorphosed spinifex textures of the randomly orientated type (Donaldson 1974).

Many of the chlorite-amphibole rocks have no obvious relict spinifex textures. They consist of small (about 0.1 mm) equant chlorite pseudomorphs after olivine set in a very fine-grained matrix of chlorite and radiating needles of tremolite (Fig. 5c) the latter presumably representing pseudomorphs after clinopyroxene. Such textures are comparable with the textures of massive or spinifex-free ultramafic komatiites, which in unaltered rocks are dominated by equant olivine crystals within a matrix of acicular clinopyroxene and glass (Arndt et al. 1977).

### ULTRAMAFIC CUMULATES

Ultramafic cumulate rocks with MgO:34–40% (volatile-free) occur in the form of discontinuous, conformable bands and lenses closely associated with the metavolcanic chlorite-amphibole rocks. In the field, the cumulate rocks are easily recognized by their chocolate-brown crusts. In these rocks, equant chlorite pseudomorphs represent original olivine megacrysts formed under conditions of slow cooling and which have settled as cumulate grains. Former olivine grain boundaries are suggested by polygonal patterns of magnetite grains and dust where the rocks resemble mesh serpentinites. Relict brown-coloured olivines are only very rarely preserved in these rocks. Other relict cumulate grains include spinel and chromite, the latter generally extensively altered to magnetite.

Metamorphic recrystallization is advanced in these rocks, and in many samples the relict primary texture and mineralogy is completely replaced by a variety of metamorphic minerals (e.g. olivine, anthophyllite, talc, magnesite and orthopyroxene). During progressive metamorphism, talc and colourless metamorphic olivine formed in earlier chlorite-antigorite areas. Olivine occurs as small individual grains (about 0.02 mm across) or as larger granular aggregates.

Anthophyllite characteristically overprints the metamorphic olivine, and occurs as acicular grains or as aggregates of grains forming fascicular bundles and bow-tie textures (Fig. 5d). Both the presence of antigorite and the formation of assemblages of olivine + anthophyllite + talc indicate that $X_{CO_2}$ was negligible during the metamorphism of these rocks (Winkler 1976 p. 160). The olivine + anthophyllite + talc assemblage may be the result of the following reactions during prograde metamorphism:

(1) antigorite = forsterite + talc

(2) talc + forsterite = anthophyllite + $H_2O$

which at a pressure of 3 kb take place over a temperature range of 560–670°C (Evans & Trommsdorff 1970). Orthopyroxene and magnesite, indicative of high $X_{CO_2}$, are only locally observed in the ultramafic rocks.

Post-metamorphic serpentinization has variably affected the ultramafic rocks. This retrograde phase of serpentinization is, however, non-penetrative and confined to local zones where the rocks are transected by veins of fibrous serpentine and carbonate.

In summary, the limited and isolated outcrops provide no clear information about the original relations between the ultramafic metavolcanics and the ultramafic rocks displaying relict cumulate textures. There is, however, no evidence that the latter are separate intrusions, and it is considered likely that these rocks are cumulates related to the volcanic chlorite-amphibole rocks. With regard to their geochemistry (e.g. in terms of $CaO$-$Al_2O_3$–$MgO$) the metavolcanic chlorite-

*Table 1.* Representative analyses of chlorite-amphibole rocks from Karasjok and some reference analyses from the literature

| *wt. %* | *1* | *2* | *3* | *4* | *5* | *6* | *7* | *8* | *9* | *10* | *11* | *12* |
|---|---|---|---|---|---|---|---|---|---|---|---|---|
| $SiO_2$ | 45.89 | 40.64 | 43.32 | 46.49 | 43.83 | 44.45 | 47.20 | 43.88 | 43.18 | 44.72 | 43.63 | 44.29 |
| $Al_2O_3$ | 4.88 | 6.33 | 6.82 | 5.89 | 5.79 | 6.28 | 5.80 | 5.92 | 6.56 | 5.56 | 6.30 | 5.96 |
| $TiO_2$ | 0.76 | 0.66 | 0.68 | 0.68 | 0.64 | 0.70 | 0.62 | 0.72 | 0.72 | 0.64 | 0.74 | 0.59 |
| $Fe_2O_3$ | 5.92 | 5.14 | 5.88 | 3.63 | 5.73 | 5.73 | 3.81 | 5.05 | 5.24 | 6.32 | 5.00 | 5.20 |
| FeO | 6.45 | 5.92 | 6.15 | 6.73 | 5.95 | 6.26 | 7.38 | 7.34 | 6.66 | 5.60 | 6.94 | 6.90 |
| MgO | 22.86 | 23.77 | 24.31 | 24.20 | 24.12 | 24.23 | 21.17 | 23.79 | 24.87 | 24.22 | 23.10 | 24.82 |
| MnO | 0.18 | 0.21 | 0.21 | 0.18 | 0.15 | 0.20 | 0.21 | 0.20 | 0.17 | 0.17 | 0.19 | 0.15 |
| CaO | 8.27 | 7.33 | 6.86 | 8.33 | 7.98 | 7.60 | 8.81 | 7.31 | 8.29 | 7.99 | 7.05 | 7.78 |
| $Na_2O$ | 0.17 | 0.27 | 0.20 | 0.21 | 0.20 | 0.08 | 0.30 | 0.13 | 0.08 | 0.43 | 0.21 | 0.20 |
| $K_2O$ | 0.12 | 0.12 | 0.11 | 0.08 | 0.12 | 0.08 | 0.09 | 0.10 | 0.08 | 0.11 | 0.10 | 0.09 |
| $P_2O_5$ | 0.01 | 0.06 | 0.03 | 0.06 | 0.05 | 0.04 | 0.04 | 0.13 | 0.08 | 0.14 | 0.11 | 0.04 |
| L.O.I. | 3.70 | 9.70 | 5.40 | 4.30 | 5.20 | 4.70 | 4.00 | 4.60 | 5.00 | 4.30 | 5.80 | 4.60 |
| Total | 99.21 | 100.15 | 99.97 | 100.78 | 99.76 | 100.35 | 99.43 | 99.17 | 100.93 | 100.20 | 99.17 | 100.62 |
| Cr (ppm) | 2428 | 2094 | 2424 | 1974 | 2048 | 1950 | 2059 | 2135 | 1882 | 2014 | 2280 | 2025 |
| Ni | 1052 | 1158 | 1200 | 955 | 1121 | 1029 | 881 | 1169 | 1050 | 899 | 1122 | 1033 |
| Co | 95 | 96 | 104 | 86 | 93 | 95 | 89 | 105 | 91 | 84 | 104 | 89 |
| Cu | 72 | 80 | 19 | 41 | 46 | 43 | 43 | 44 | 17 | 46 | 113 | 68 |
| Zr | 16 | 25 | 36 | 30 | 32 | 19 | 23 | 40 | 43 | 23 | 22 | 32 |
| Y | 7 | 7 | 8 | 7 | 8 | 6 | 7 | 9 | 7 | 7 | 7 | 6 |
| Sc | – | – | – | 25 | 25 | – | 25 | – | – | 28 | – | 24 |
| V | 203 | 169 | 209 | 168 | 172 | 168 | 184 | 175 | 171 | 177 | 202 | 162 |

1–13: Metavolcanic chlorite-amphibole rocks
14–15: Pillowed chlorite-amphibole rocks.
A. Means and standard deviations of analyses 1–15.
B. Analyses A recalculated on a volatile-free basis.
16–19: Cumulate chlorite-amphibole rocks.
C. Means and standard deviations of analyses 16–19.
D. Analyses C recalculated on a volatile-free basis.
E. Picritic komatiites from Finnish greenstone belts (5 analyses, Blais et al. 1979).
F. Spinifex-textured komatiites, Scotia, Western Australia (32 analyses, Stolz & Nesbitt 1981).

* total iron as FeO — – not analysed
o total iron as $Fe_2O_3$ — X not detected

amphibole rocks and the recrystallized cumulates fall in the fields for the flow and cumulate zones, respectively, of komatiitic flows (Fig. 7).

## The mafic metavolcanics

Mafic metavolcanics occur as amphibolites of basaltic composition (Table 2). The majority of these rocks are fine- to medium-grained, well-foliated hornblende schists which rarely preserve any primary features. Presumably, they represent massive basaltic flows. Pillow structures have been observed, however, in a few outcrops.

Some amphibolites are distinctly plagioclase-striped and are probably metagabbros. Banded amphibolites with thin calcareous bands are sometimes present, and may represent original tuffaceous rocks or impure limey sediments.

| *13* | *14* | *15* | *A* | *B* | *16* | *17* | *18* | *19* | *C* | *D* | *E* | *F* |
|---|---|---|---|---|---|---|---|---|---|---|---|---|
| 43.05 | 41.74 | 43.70 | 44.00 (1.61) | 46.66 | 39.78 | 39.90 | 40.86 | 37.68 | 39.55 (1.16) | 44.36 | 46.85 | 44.64 |
| 5.82 | 5.27 | 5.23 | 5.89 (0.50) | 6.24 | 2.55 | 2.66 | 3.31 | 2.36 | 2.72 (0.35) | 3.05 | 8.08 | 6.68 |
| 0.56 | 0.71 | 0.67 | 0.67 (0.05) | 0.71 | 0.33 | 0.26 | 0.21 | 0.53 | 0.33 (0.12) | 0.37 | 0.40 | 0.40 |
| 5.14 | 1.42 | 0.88 | 4.67 (0.55) | 4.95 | 4.15 | 5.10 | 6.85 | 9.36 | 6.36 (1.98) | 7.13 | – | 11.77[0] |
| 5.10 | 8.71 | 9.11 | 6.74 (1.04) | 7.15 | 6.12 | 5.10 | 5.30 | 5.08 | 5.40 (0.42) | 6.06 | 10.75* | – |
| 25.48 | 23.05 | 23.14 | 23.80 (1.00) | 25.25 | 31.12 | 34.65 | 31.58 | 33.51 | 32.71 (1.43) | 36.68 | 26.01 | 29.40 |
| 0.20 | 0.19 | 0.81 | 0.19 (0.02) | 0.20 | 0.18 | 0.22 | 0.25 | 0.17 | 0.21 (0.03) | 0.23 | 0.17 | 0.13 |
| 7.98 | 9.51 | 9.17 | 8.01 (0.72) | 8.50 | 2.29 | 0.58 | 2.38 | 1.83 | 1.77 (0.71) | 1.99 | 7.45 | 6.05 |
| 0.10 | x | x | 0.17 (0.11) | 0.18 | 0.04 | x | x | x | 0.01 (0.01) | 0.01 | 0.18 | 0.38 |
| 0.10 | 0.08 | 0.04 | 0.09 (0.02) | 0.10 | x | 0.06 | 0.05 | 0.11 | 0.06 (0.04) | 0.07 | 0.03 | 0.13 |
| 0.10 | 0.04 | 0.07 | 0.06 (0.03) | 0.06 | 0.05 | 0.06 | 0.02 | 0.02 | 0.04 (0.02) | 0.04 | 0.07 | 0.03 |
| 6.30 | 9.40 | 8.50 | 5.70 (1.88) | – | 13.26 | 11.40 | 9.70 | 10.50 | 11.21 (1.32) | – | – | – |
| 99.93 | 100.12 | 100.69 | 99.99 | 100.00 | 99.87 | 99.99 | 100.51 | 101.15 | 100.37 | 99.99 | 99.99 | 99.61 |
| 1504 | 2481 | 2408 | 2113 (250) | 2113 | 3901 | 3451 | 3948 | 3452 | 3688 (237) | 3688 | – | 3325 |
| 928 | 854 | 878 | 1022 (112) | 1022 | 1679 | 1838 | 1206 | 1520 | 1560 (233) | 1560 | – | 1354 |
| 83 | 91 | 92 | 93 (7) | 93 | – | 122 | 124 | 125 | 123 (1.24) | 123 | – | – |
| 18 | 185 | 187 | 68 (52) | 68· | 35 | 48 | 32 | 194 | 77 (67.6) | 77 | – | – |
| 34 | 27 | 25 | 28 (7) | 28 | – | 12 | 15 | 26 | 17 (6) | 17 | – | – |
| 7 | 4 | 7 | 7 (1) | 7 | – | 4 | 4 | 6 | 5 (0.94) | 5 | – | – |
| 21 | – | 25 | 25 (2) | 25 | – | 12 | – | – | 12 (0) | 12 | – | – |
| 140 | 205 | 199 | 180 (19) | 180 | – | 73 | 72 | 10 | 84 (16) | 84 | – | – |

The analyses reported in Table 2 are only from homogeneous hornblende schists considered to be of volcanic origin. The texture of these amphibolites is entirely metamorphic, and they are characterized by the mineral assemblage:
*Albite/oligoclase + hornblende ± quartz ± epidote ± biotite ± chlorite ± garnet* which is attributable to metamorphic recrystallization under upper greenschist to low amphibolite facies conditions.

Analyses of the mafic metavolcanics are presented in Table 2 and compared with analyses from the literature. Plotted in terms of $Na_2O + K_2O$, MgO and $FeO_t$ (Fig. 6), the mafic metavolcanics would be located in the tholeiitic field as defined by Irvine & Baragar (1971). Compared with modern ocean-ridge and island-arc tholeiites, however, the Karasjok mafic metavolcanics have lower $Al_2O_3$ and higher total iron; they resemble modern oceanic ferrobasalts and Archaean iron-rich tholeiites.

## Geochemistry

### SAMPLING AND ANALYTICAL METHODS

About sixty samples of mafic and ultramafic metavolcanics from the area north of Karasjok have been collected. Highly altered and oxidized samples were excluded, and the remaining samples were trimmed with a diamond saw and washed before further treatment. All major elements except sodium were analyzed by X-ray fluorescence (XRF) employing fused glass beads. Powder briquettes were used for the determination of sodium and the trace elements. During the course of the analyses, the U.S.G.S. standards BCR–1 and AGV–1 as well as the NIM–P standard were monitored. A number of duplicate $Na_2O$ and MgO determinations

*Table 2.* Representative analyses of mafic metavolcanics from Karasjok and some reference analyses from the literature

| *wo. %* | *1* | *2* | *3* | *4* | *5* | *6* | *7* | *8* | *9* | *10* | *11* |
|---|---|---|---|---|---|---|---|---|---|---|---|
| $SiO_2$ | 48.98 | 48.72 | 51.71 | 56.13 | 49.84 | 51.24 | 49.87 | 47.93 | 48.04 | 49.43 | 49.28 |
| $Al_2O_3$ | 13.42 | 13.40 | 13.18 | 12.09 | 13.41 | 14.79 | 13.60 | 14.27 | 14.48 | 13.99 | 13.24 |
| $TiO_2$ | 1.25 | 1.24 | 1.23 | 1.16 | 1.00 | 1.21 | 1.06 | 1.39 | 1.96 | 1.14 | 1.84 |
| $Fe_2O_3$ | 1.56 | 1.49 | 1.97 | 0.55 | 0.86 | 2.24 | 1.71 | 2.49 | 2.70 | 1.31 | 1.52 |
| FeO | 11.52 | 10.19 | 9.90 | 9.65 | 11.99 | 7.85 | 10.08 | 10.80 | 10.80 | 11.88 | 13.00 |
| MgO | 7.20 | 7.07 | 6.62 | 6.15 | 7.60 | 7.44 | 7.61 | 6.97 | 6.20 | 7.03 | 6.16 |
| MnO | 0.23 | 0.20 | 0.19 | 0.16 | 0.24 | 0.16 | 0.23 | 0.24 | 0.23 | 0.20 | 0.22 |
| CaO | 9.28 | 11.40 | 10.40 | 7.80 | 9.22 | 10.11 | 10.54 | 10.21 | 10.21 | 9.60 | 9.55 |
| $Na_2O$ | 2.80 | 2.04 | 1.42 | 4.25 | 2.07 | 2.99 | 1.70 | 2.01 | 3.17 | 2.36 | 2.00 |
| $K_2O$ | 0.51 | 0.58 | 0.44 | 0.26 | 0.49 | 0.45 | 0.31 | 0.37 | 0.32 | 0.41 | 0.41 |
| $P_2O_5$ | 0.12 | 0.07 | 0.12 | 0.09 | 0.10 | 0.13 | 0.08 | 0.12 | 0.20 | 0.09 | 0.16 |
| L.O.I. | 1.80 | 2.20 | 2.50 | 1.50 | 2.10 | 1.50 | 2.30 | 2.10 | 1.60 | 1.90 | 2.00 |
| Total | 98.67 | 98.60 | 99.68 | 99.79 | 98.92 | 100.11 | 99.09 | 98.90 | 99.91 | 99.34 | 99.38 |
| Cr (ppm) | 132 | 146 | 210 | 213 | 101 | 183 | 225 | 175 | 140 | 180 | 89 |
| Ni | 54 | 58 | 73 | 68 | 46 | 65 | 77 | 59 | 35 | 68 | 20 |
| Co | 86 | 75 | 74 | 66 | 80 | 64 | 76 | 82 | 81 | 84 | 84 |
| Cu | 188 | 181 | 217 | 175 | 169 | 169 | 187 | 164 | 174 | 208 | 157 |
| Zr | 47 | 45 | 49 | 98 | 38 | 54 | 42 | 51 | 78 | 46 | 72 |
| Y | 13 | 14 | 13 | 14 | 13 | 16 | 13 | 15 | 19 | 14 | 20 |
| Sc | – | – | – | – | – | – | – | – | – | – | – |
| V | 322 | 296 | 291 | 247 | 275 | 270 | 270 | 324 | 392 | 295 | 392 |

1–16: Mafic metavolcanics.

A. Means and standard deviations of analyses 1–16.
B. Analyses A recalculated on a volatile-free basis.
C. Fe-rich tholeiites from Yakabindie, Western Australia (20 analyses, Naldrett & Turner 1977).
D. Tholeiites from Scotia, Western Australia (26 analyses, Stolz & Nesbitt 1981).
E. Tholeiites from Finnish greenstone belts (11 analyses, Blais et al. 1978).
F. Modern oceanic tholeiites (161 analyses, Hyndman 1972, p. 171).

* total iron as FeO — not analysed
o total iron as $Fe_2O_3$ x not detected

were obtained by atomic absorption to check the validity of the XRF $Na_2O$ and MgO determinations. Water and carbon dioxide were determined by conventional techniques, and constitute together with other volatiles the L.O.I. values. FeO was determined by titration with potassium dichromate. Representative analyses are presented in Tables 1 and 2.

## ALTERATION EFFECTS

Secondary alteration and regional metamorphism may change the primary compositions of volcanic rocks considerably. The main results from studies of alteration have been summarized by Condie (1981, p. 71). Significant changes may take place in the concentrations of $SiO_2$, CaO, $Al_2O_3$, MgO, $K_2O$, $H_2O$, $CO_2$ and the $Fe^{3+}/Fe^{2+}$ ratio during progressive alteration and metamorphism. On the other hand, little or no changes are reported for the concentations of $TiO_2$, total

| *12* | *13* | *14* | *15* | *16* | *A* | *B* | *C* | *D* | *E* | *F* |
|---|---|---|---|---|---|---|---|---|---|---|
| 48.40 | 47.69 | 54.23 | 49.63 | 50.62 | 50.11 (2.23) | 51.47 | 51.64 | 49.11 | 50.90 | 49.30 |
| 15.08 | 15.65 | 12.83 | 13.23 | 13.64 | 13.77 (0.87) | 14.14 | 13.70 | 14.99 | 14.04 | 15.20 |
| 1.12 | 1.79 | 0.88 | 1.54 | 1.71 | 1.34 (0.31) | 1.37 | 1.61 | 1.07 | 1.98 | 1.80 |
| 2.82 | 2.47 | 2.95 | 1.86 | 4.10 | 2.04 (0.85) | 2.09 | – | $13.37^{0}$ | – | 2.40 |
| 10.01 | 9.72 | 9.25 | 11.34 | 10.30 | 10.51 (1.20) | 10.79 | $14.90^{\bullet}$ | – | $14.94^{\bullet}$ | 8.00 |
| 7.28 | 5.64 | 5.77 | 7.12 | 5.06 | 6.68 (0.74) | 6.86 | 4.09 | 7.03 | 5.63 | 8.30 |
| 0.22 | 0.17 | 0.28 | 0.21 | 0.21 | 0.21 (0.03) | 0.21 | 0.30 | 0.23 | 0.24 | 0.17 |
| 9.63 | 9.40 | 8.36 | 10.47 | 8.69 | 9.68 (0.87) | 9.94 | 8.96 | 11.68 | 8.90 | 10.80 |
| 2.55 | 2.80 | 1.63 | 2.28 | 3.21 | 2.45 (0.70) | 2.52 | 2.37 | 2.21 | 2.81 | 2.60 |
| 0.85 | 0.79 | 0.75 | 0.27 | 0.37 | 0.47 (0.17) | 0.48 | 0.28 | 0.30 | 0.37 | 0.24 |
| 0.12 | 0.22 | 0.09 | 0.14 | 0.20 | 0.13 (0.04) | 0.13 | – | 0.10 | 0.19 | 0.21 |
| 2.40 | 2.50 | 2.20 | 2.20 | 1.50 | 2.01 (0.33) | – | – | 1.38 | – | – |
| 100.48 | 98.84 | 99.22 | 100.29 | 99.61 | 99.40 | 100.00 | 97.85 | 101.47 | 100.00 | 99.02 |
| 97 | 189 | 323 | 162 | 105 | 166 (58) | 166 | – | 246 | – | – |
| 83 | 47 | 103 | 57 | 42 | 59 (19) | 59 | – | 129 | – | – |
| 79 | 66 | 77 | 79 | 91 | 77 (7) | 77 | – | – | – | – |
| 181 | 216 | 164 | 232 | 146 | 183 (23) | 183 | – | – | – | – |
| 25 | 67 | 37 | 40 | 66 | 53 (18) | – | – | – | – | – |
| 12 | 18 | 9 | 15 | 14 | 14 (14) | – | – | – | – | – |
| – | – | – | – | – | – | – | – | – | – | – |
| 230 | 391 | 211 | 342 | 361 | 361 (306) | 306 | – | – | – | – |

Fe and the trace and rare-earth elements. Notable exceptions, however, are Rb, Sr, Ba, and the LREE (Frey et al. 1974). In ultramafic rocks, serpentinization and carbonatization are common alteration phenomena which can significantly modify the original major-element chemistry. During these processes, there appears to be a general decrease in $SiO_2$, $Al_2O_3$, MgO, $Na_2O$, $K_2O$, CaO and $Fe^{2+}$, an increase in $H_2O$ and $CO_2$, and small enrichments of the LREE and $TiO_2$ (Condie 1981).

In general, the Karasjok metavolcanics display a wide range in their $Fe_2O_3$/FeO ratios from that of unaltered igneous rocks in the compact and non-schistose rocks to ratios near or greater than unity in the more foliated varieties, suggesting oxidation of FeO during deformation. In the ultramafic chlorite-amphibole rocks the high L.O.I. values (up to 13%; Table 1) must be taken as an indication of alteration. However, many of the high L.O.I. values are probably associated with the hydration of the original olivine-dominated assemblages of the ultramafic rocks. Carbonatization and retrograde serpentinization are rare, and are restricted to some of the most ultramafic (MgO>35%) cumulate rocks.

Another indication of alteration is seen in the scatter of points in the major-oxide variation diagrams, particularly for $Na_2O$ and $K_2O$ (Figs. 8 & 9). The other major elements define trends which can be meaningfully related to theoretical petrogenetic models (i.e. fractional crystallization), indicating that the analytical data largely reflect original igneous variations.

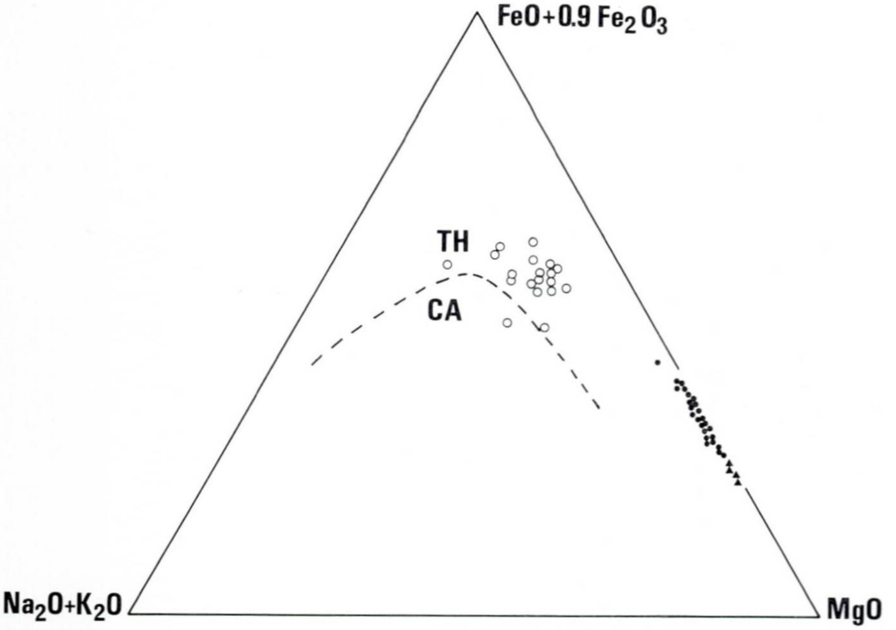


*Fig. 6.* AFM-diagram for the Karasjok metavolcanics. Both the mafic and the ultramafic metavolcanics fall within the tholeiitic field according to Irvine and Baragar (1971), but there is no obvious compositional continuum between the two groups. *Open circles:* mafic metavolcanics, *filled circles:* ultramafic metavolcanics, *filled triangles:* ultramafic cumulates.

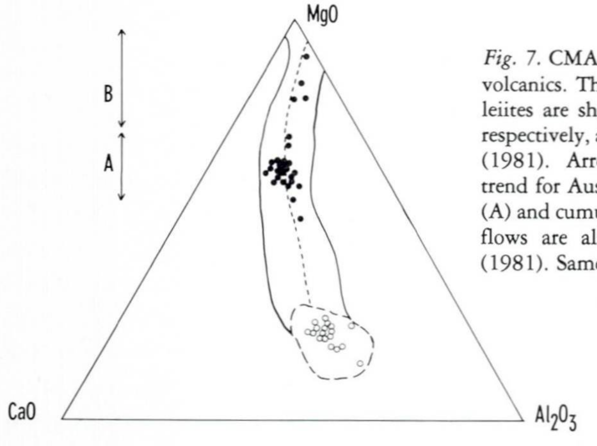


*Fig. 7.* CMA-diagram for the Karasjok metavolcanics. The fields for komatiites and tholeiites are shown by solid and broken lines, respectively, and are taken from Marston et al. (1981). Arrows indicate the fractionation trend for Australian komatiites, and the flow (A) and cumulate (B) zones for the komatiite-flows are also taken from Marston et al. (1981). Same symbols as in Fig. 6.

## MAJOR–ELEMENT CHEMISTRY

The location of the Karasjok metavolcanics in the conventional AFM and CMA triangles is shown in Figs. 6 & 7. The mafic metavolcanics are located in the tholeiitic fields in both the AFM and CMA diagrams, and in the CMA triangle the ultramafic chlorite-amphibole rocks fall within the field for the komatiite series (Condie 1981, Fig. 3–6). There is, however, no obvious compositional continuum between the ultramafic and mafic metavolcanics. In the AFM diagram, the ultramafic chlorite-amphibole rocks are located close to the $FeO_t$–MgO side, reflecting their paucity in alkalies.

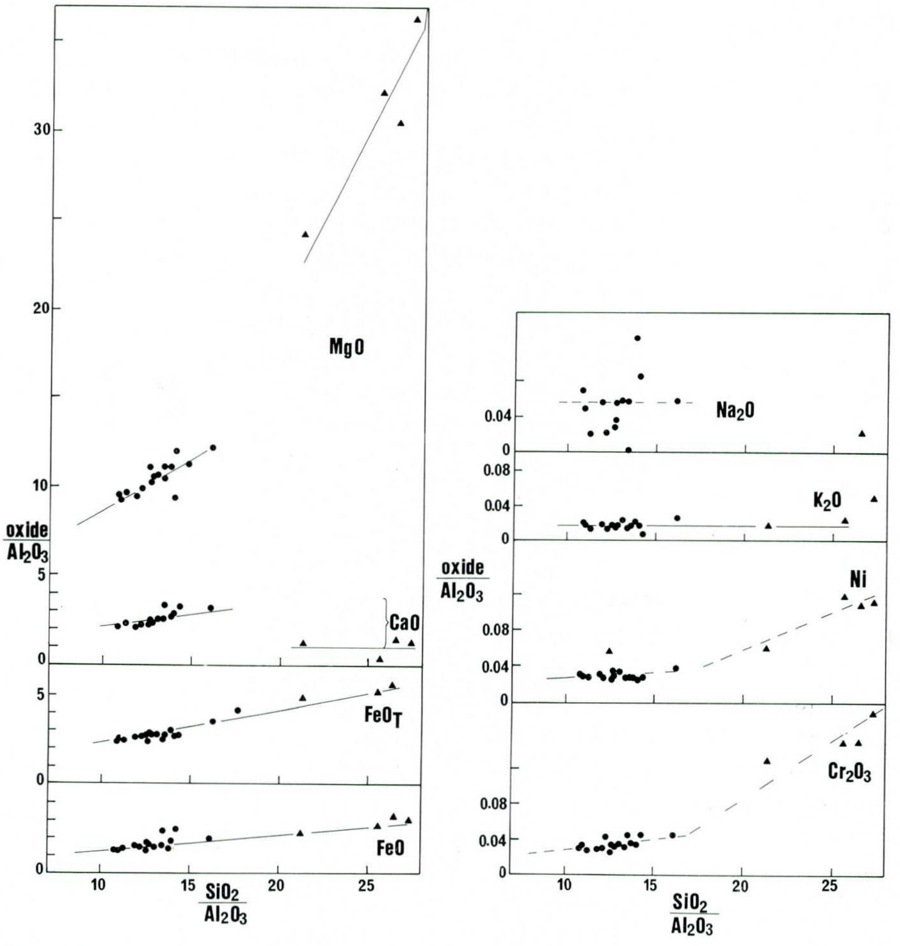


*Fig. 8.* Molar ratio variation diagrams for the chlorite-amphibole rocks. *Filled circles:* metavolcanic rocks, *filled triangles:* cumulate rocks.

Plotted in terms of $CaO–Al_2O_3–MgO$ (Fig. 7), the ultramafic volcanic and cumulate rocks define a trend characterized by decreasing MgO with near constant $CaO/Al_2O_3$. This suggests that fractionation of olivine was the dominant factor in the compositional variation of these rocks. For the cumulate rocks the change in trend away from the CaO–MgO side probably reflects the loss of CaO from these rocks due to serpentinization. Compared with komatiitic rocks elsewhere, the rocks from Karasjok plot in the fields for the flow zones and cumulate zones, respectively, in the CMA triangle (Fig. 7).

The major-element variation for the Karasjok metavolcanics is illustrated in cartesian plots of the molecular proportions of two oxides normalized against the molecular proportion of a third component (see Pearce 1968,1969). Assuming a fractional crystallization model, components that are extracted from the system will generate linear trends with slopes that indicate the rate at which the components are fractionated relative to that employed as divisor. Components that retain constant concentrations relative to the divisor will define linear trends with zero slopes. For the ultramafic rocks, $Al_2O_3$ has been chosen as the normalizing parameter. $Al_2O_3$ is largely fractionated into the liquid during the differentiation of ultramafic magmas, and tends to remain immobile during metamorphism (McQueen 1981). It is also present in sufficient amounts to avoid problems connected with analytical error.

For the ultramafic chlorite-amphibole rocks, most major elements as well as Ni and Cr generate straight lines with different slopes for the volcanic and the cumulate rocks (Fig. 8). The fractionating major elements are Mg, Fe and only minor Ca, which shows the importance of olivine fractionation. The break in slope in the MgO *vs.* $SiO_2$ and Ni *vs.*$SiO_2$ plots for the cumulate rocks reflects the concentration of these components in cumulate olivine. The slope of the MgO *vs.*$SiO_2$ line (about 2.14) is, however, too large to be explained by concentration of MgO in olivine alone since the fractionation of pure forsterite would produce a MgO *vs.*$SiO_2$ line with a slope of 2. This requires the concentration of the remaining MgO in an additional cumulate phase, probably chromite or picotite (cf. p. 40).

If one allots all the fractionating FeO to form olivine, a minimum value of $Fo_{91}$ for the fractionating olivine is indicated by the slope of the $FeO_t$ *vs.* $SiO_2$ line. For the mafic metavolcanics, (Fig. 9), the MgO *vs.* $SiO_2$ and CaO *vs.* $SiO_2$ plots normalized against $Al_2O_3$ define parallel linear trends attributable to fractionation of clinopyroxene. The additional involvement of an iron-rich (opaque) phase is also indicated by the trend in the FeO *vs.* $SiO_2$ plot. An assessment of the molar values normalized against some other component (e.g. $K_2O$) suggests that $Al_2O_3$ was not incompatible during the differentiation of the mafic metavolcanics, as the slope of the $Al_2O_3$ *vs.* $SiO_2$ line indicates $Al_2O_3$ fractionation.

The molar ratio plots, particularly in terms of MgO *vs.* $SiO_2$, reveal no obvious continuity of the linear trends generated by the ultramafic and mafic metavolcanics. This may be taken as an indication of the presence of two fractionating silicate liquids.

The analyses of phenocryst-free, pillowed or microspinifex-textured ultramafics display a rather narrow compositional variation (Table 1) and tend to concentrate in a restricted field in the CMA triangle (Fig. 7). It is believed that the average composition of these rocks (about 25% MgO volatile free) is representative of the primary ultramafic liquid composition. The ultramafic rocks covering the MgO-range from 21–39% may have formed from this parent by crystal fractionation, the accumulation of olivine and chromite having formed the high-magnesian cumulates, and the derivative liquid having formed the less magnesian volcanics.

A likely representative of the primary mafic liquid composition is the composition of the rocks richest in MgO (about 8% volatile-free). Judging from the molar ratio plots, the general differentiation of these rocks was controlled by clinopyroxene and minor plagioclase fractionation. The influence of an opaque phase rich in iron is also indicated. Possible cumulates related to the mafic metavolcanics occur in the form of associated lenses of metagabbro.

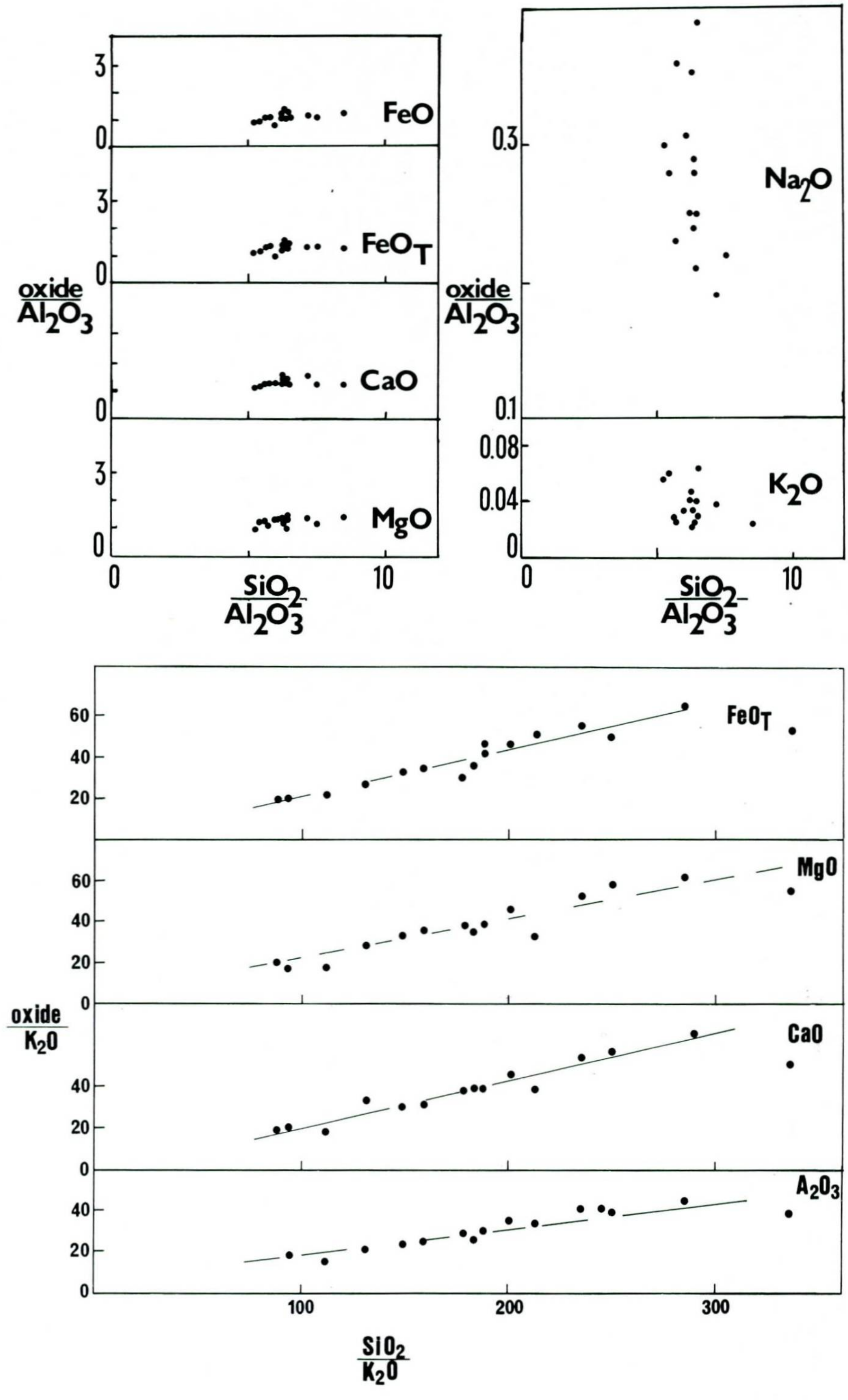


*Fig. 9.* Molar ratio variation diagrams for the mafic metavolcanics.

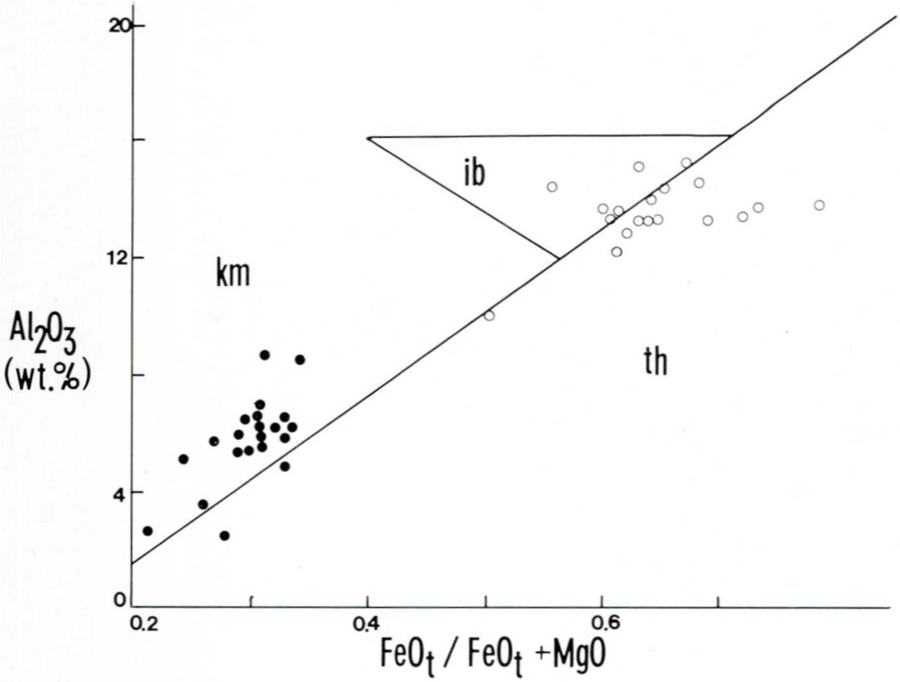


*Fig. 10.* $Al_2O_3$ *vs.* $FeO_t/(FeO_t + MgO)$ diagram for the Karasjok metavolcanics. Km: komatiite field; th: tholeiite field; ib: field of intermediate basalts according to Naldrett & Goodwin (1977). Same symbols as in Fig. 8.

A general feature of many Archaean greenstone belts appears to be the association of a tholeiitic and a komatiitic volcanic series within the lower stratigraphic levels of the succession (e.g. Arndt et al. 1977, Blais et al. 1978, Jahn et al. 1980, Condie 1981). In the $FeO_t/(FeO_t + MgO)$ *vs.* $Al_2O_3$ diagram (Arndt et al. 1977), which is frequently used to discriminate between basaltic rocks of the komatiite spectrum and basaltic tholeiites, the Karasjok mafic volcanics define a trend across the komatiite-tholeiite dividing line (Fig. 10). Many Archaean tholeiites plot in the high $Al_2O_3$ low $FeO_t/(FeO_t + MgO)$ field (Naldrett & Goodwin 1977, Nesbitt et al. 1979). In a modified $FeO_t/(FeO_t + MgO)$ *vs.* $Al_2O_3$ plot proposed by Naldrett & Goodwin (1977), such tholeiites with high $TiO_2$ were termed intermediate tholeiites and considered to form a transition to the typical iron-rich tholeiites.

$TiO_2$*vs.*$Al_2O_3$, $TiO_2$ *vs.* $SiO_2$ or $TiO_2$ *vs.* MgO diagrams are often used to discriminate between komatiitic and tholeiitic series (Arndt et al. 1977, Blais et al. 1978), as for any value of $Al_2O_3$, $SiO_2$ or MgO the $TiO_2$ contents of tholeiites exceed that of komatiites. In Fig. 11, the $TiO_2$ *vs.* $SiO_2$ and $TiO_2$ *vs.* MgO plots for the Karasjok metavolcanics are shown. The ultramafic chlorite-amphibole rocks and the mafic metavolcanics are clearly discriminated on these plots as members of a komatiitic and a tholeiitic series, respectively, separated at a $TiO_2$ value of about 0.9%.

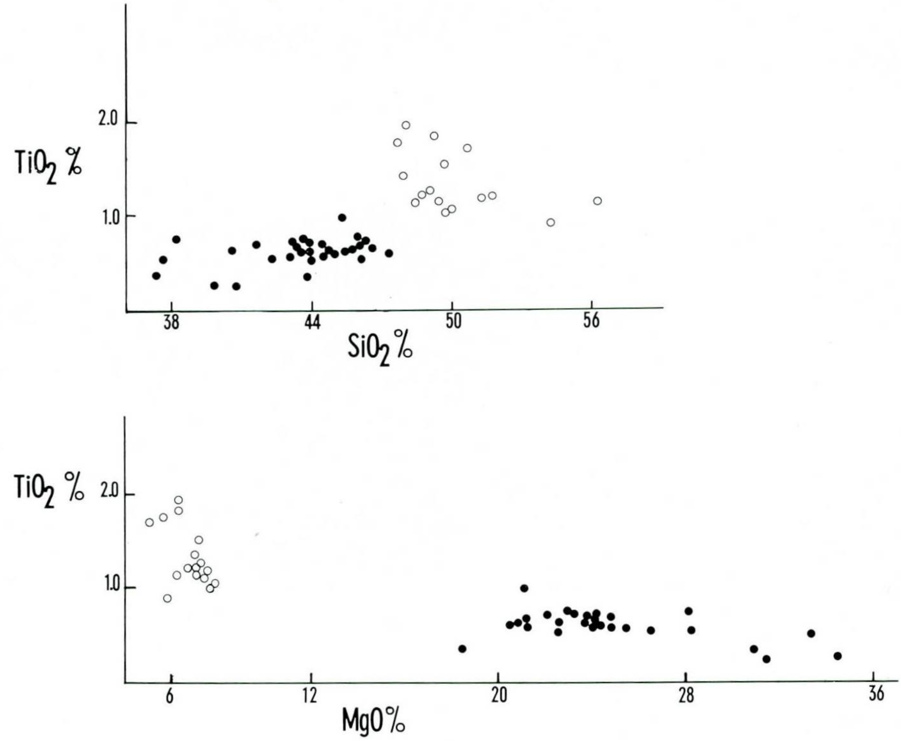


*Fig. 11.* $TiO_2$ *vs.* $SiO_2$ and $TiO_2$ *vs.* MgO diagrams for the Karasjok metavolcanics. A komatiitic and a tholeiitic series are clearly discriminated on these diagrams by a $TiO_2$ value of about 0.9. Same symbols as in Fig. 8.

The distinct bimodal grouping is illustrated by the $TiO_2$ *vs.*MgO plot, which highlights the absence of rocks with 8–20% MgO. This bimodality appears to be a primary feature. Alternatively, the absence of intermediate compositions could be the result of element mobilization due to alteration and metamorphism. An assessment of the molar ratio variation diagrams (Figs. 8 & 9), however, suggests that no mobilization of magnesium has taken place to an extent which could account for the compositional gap between the members of the komatiitic and tholeiitic series. Moreover, both compact non-foliated and metamorphic-textured metavolcanics have been analysed, which makes inadequate sampling unlikely as an explanation for the bimodal grouping.

TRACE ELEMENT VARIATIONS

*Ni, Co and Cr.* In the komatiitic rocks, there is an enrichment of Ni, Co and Cr in the cumulate rocks (Table 1, Figs. 8 & 12). For Ni and Co, this is consistent with the concentration of these elements in olivine during the first stages of crystallization. The enrichment of Cr in the high-magnesian cumulate rocks is opposite to the trend observed for the Munro Township komatiites by Arndt et al. (1977), where the highest Cr contents are in the spinifex-textured rocks with

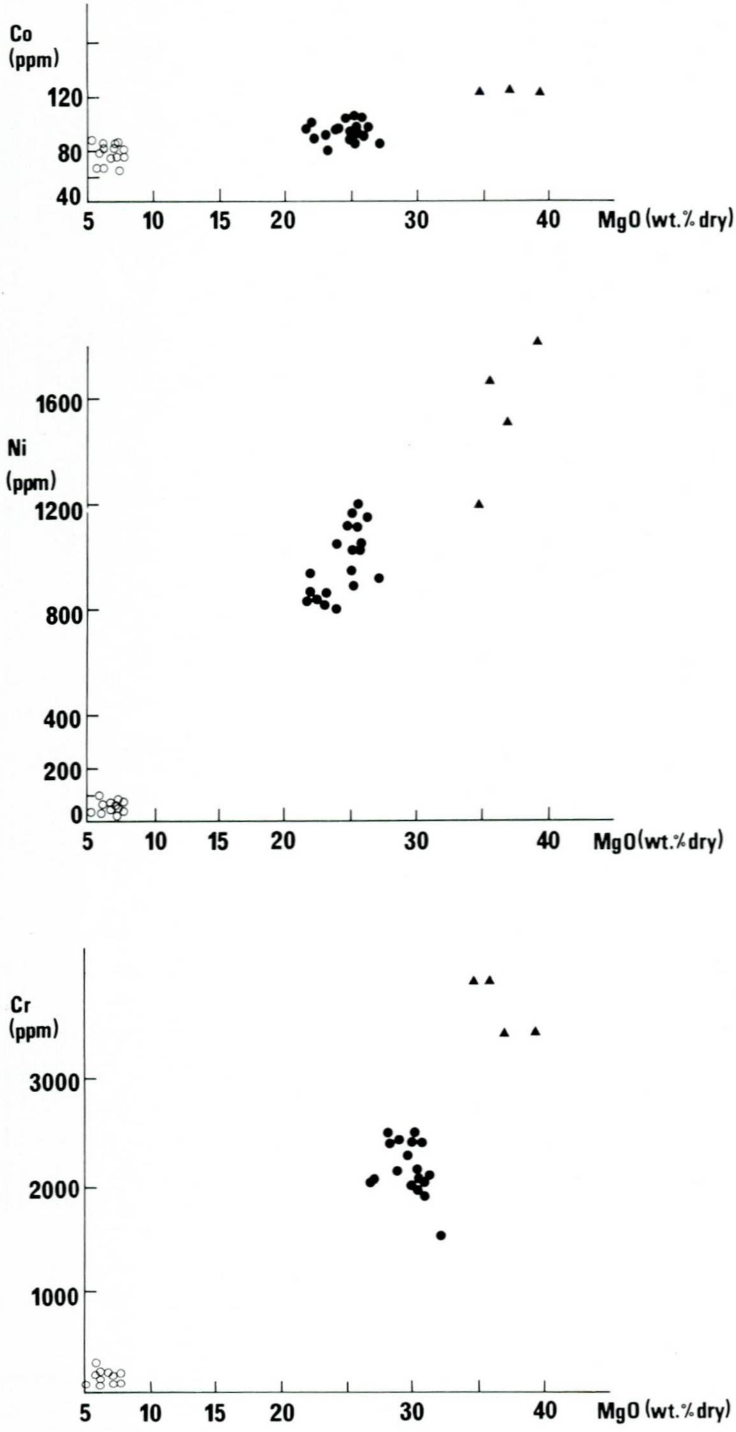


*Fig. 12.* Variation diagrams of Ni, Cr and Co against MgO (wt.% dry) for the Karasjok metavolcanics. Same symbols as in Fig. 8.

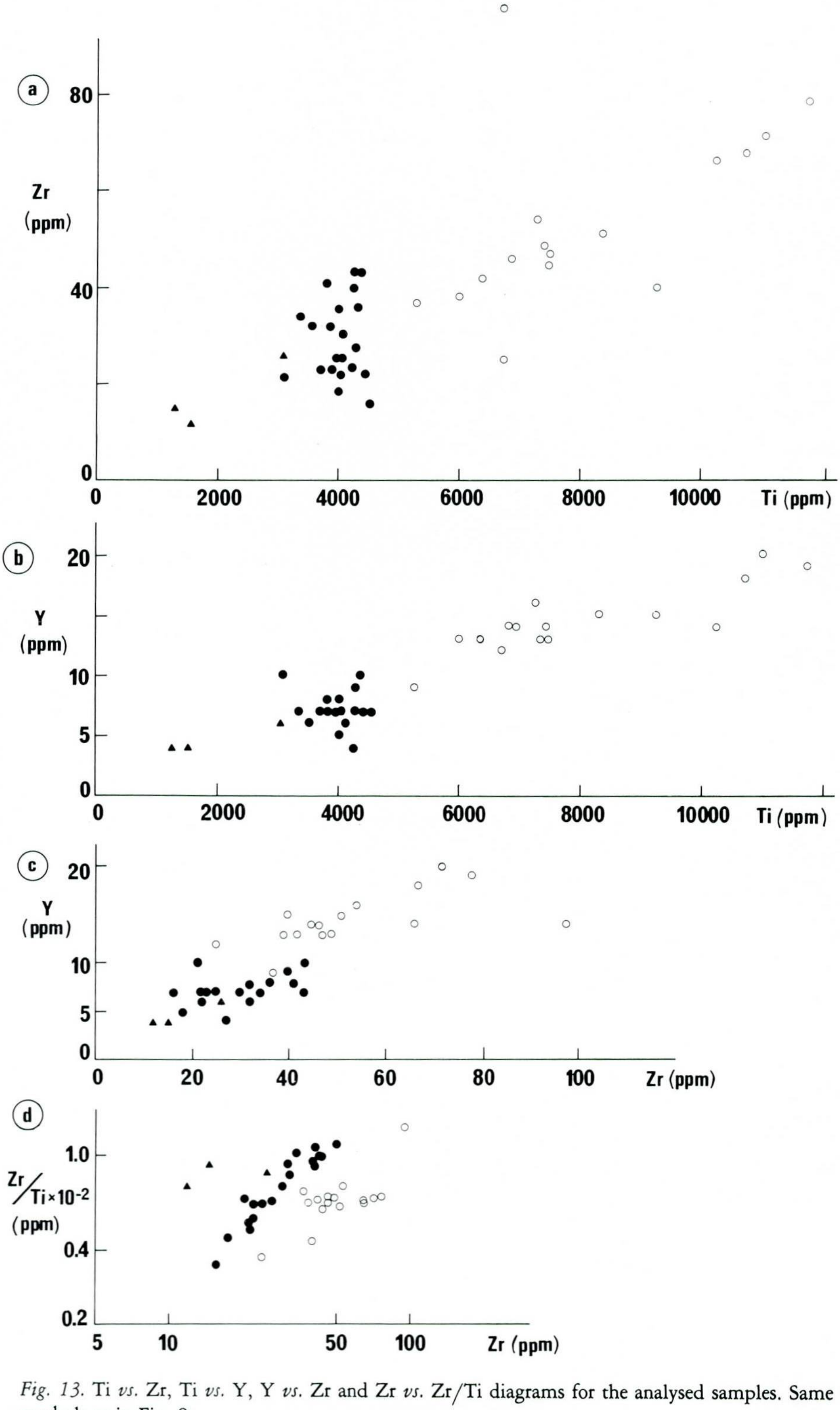


*Fig. 13.* Ti *vs.* Zr, Ti *vs.* Y, Y *vs.* Zr and Zr *vs.* Zr/Ti diagrams for the analysed samples. Same symbols as in Fig. 8.

intermediate MgO contents (18–25%). In the Finnish greenstone belts, however, a trend similar to that for the Karasjok komatiites has been described by Jahn et al. (1980). Although olivine in komatiites may contain significant amounts of Cr, the olivine/melt distribution coefficient for Cr is apparently too low to explain the enrichment of Cr in the cumulate rocks by concentration of Cr in olivine alone. Hence, separation and accumulation of chromite or chrome-spinel in addition to olivine fractionation seems necessary to account for the observed Cr-concentrations (Jahn et al. 1980). In the komatiitic cumulates from Karasjok, the presence of an additional Mg-bearing phase containing Cr is suggested by the slopes of the MgO *vs.* $SiO_2$ and MgO *vs.* $Cr_2O_3$ lines in the molar ratio plots (Fig. 8).

*Ti, Zr and Y.* On Ti *vs.* Zr, Ti *vs.* Y and Zr *vs.* Y plots, many komatiitic rocks and basalts generate chondritic straight-line trends, suggesting the incompatible behaviour of these elements during partial melting (Nesbitt & Sun 1976). The Ti *vs.* Zr plot (Fig. 13a) defines a linear trend with a Ti/Zr ratio of 145. This is significantly higher than the chondritic Ti/Zr ratio of 110 found by Nesbitt & Sun (1976), but is close to the ratio of 140 for the Finnish greenstone-belt komatiites and tholeiites reported by Jahn et al. (1980).

In the Zr-Y plot, the komatiitic and tholeiitic rocks define a trend with a Zr/Y ratio of about 4.3. This is 1.8 times the chondritic value, indicating Y depletion or Zr enrichment. In this plot, the mafic metavolcanics are scattered, particularly at high Zr concentrations. Such variations in the Zr/Y ratio could be attributable to derivation from an enriched mantle source (Pearce & Norry 1979).

The Ti-Y plot defines a Ti/Y ratio of about 480. This is again higher than the chondritic ratio of 290 (Nesbitt & Sun 1976), and could be related to the retention of Y in some residual phase (garnet) during partial melting, or to a mantle source enriched in Ti. Preliminary data on Sc from the komatiitic rocks, however, indicate a strong Sc depletion with Ti/Sc ratios in the order of twice the chondritic Ti/Sc ratio. This, together with the high $CaO/Al_2O_3$ ratios (average 1.3) in the komatiitic rocks indicates that garnet, either as a residual or cumulate phase, may have had a major influence on the genesis of these rocks.

The Karasjok komatiitic rocks also have high Ti/V ratios (average 22.5) and low $Al_2O_3/TiO_2$ ratios (average 8.8), and are thus in many respects similar to the Barberton or aluminium-depleted periodotitic komatiites of Nesbitt et al. (1979). The involvement of garnet appears necessary to explain this type of komatiite (Nesbitt et al. 1979, Nesbitt & Sun 1980).

The Zr *vs.* Zr/Ti plot (Fig. 13d) shows two separate trends for the Karasjok komatiitic and mafic metavolcanics. The komatiitic rocks fall along the trend for komatiites dominated by olivine and minor spinel fractionation (Nisbett & Chinner 1981). The mafic metavolcanics define a subparallel trend at higher Zr concentrations.

## Conclusions

On the basis of geological and petrochemical evidence, it is suggested that the metavolcanic rocks of the Karasjok greenstone belt can be divided into two general groups: (a) ultramafic (MgO: 21–39% volatile-free) chlorite-amphibole rocks; and (b) mafic (MgO:5–8% volatile-free) metavolcanics. The ultramafic chlorite-amphibole rocks include volcanics and related cumulates which satisfy existing definitions of komatiites as employed by Arndt & Brooks (1980) and Arndt & Nisbet (1982). The mafic metavolcanics are amphibolites with tholeiitic geochemical affinities and resemble Archaean intermediate and iron-rich tholeiites.

The geochemical data suggest no obvious genetic relationship by fractional crystallization between the ultramafic komatiites and the mafic metavolcanics. It is suggested that the range of ultramafic komatiites and the mafic volcanics formed by fractionation of two parent liquids, with compositions of about 25% and 8% MgO, respectively. On the other hand, plots of incompatible elemental ratios generate straight and continuous trends for the ultramafic komatiites and the mafic volcanics, which may reflect the derivation of these rocks from the same source region by various degrees of partial melting.

The ultramafic komatiites and the mafic volcanics can be distinguished as members of a komatiitic and a tholeiitic series, respectively, by plotting $TiO_2$ against $SiO_2$ or MgO. The high-Mg volcanic rocks of the komatiite association are found almost exclusively in Archaean greenstone belts. The existence of similar rocks in the Karasjok greenstone belt provides a link with the well established Archaean (2.6–2.75 Ga.) greenstone belts in eastern and northern Finland, where komatiitic and tholeiitic volcanic rocks are important components (Blais et al. 1978). Associated with ultramafic komatiites in both belts are exhalative-sedimentary Fe-Mn formations typical of the Archaean. These features as well as other lithostratigraphical similarities suggest that the Karasjok greenstone belt represents the northern extension of the Finnish or Fennoscandian greenstone belt association. An Archaean age is therefore considered more appropriate for the Karasjok greenstone belt than the traditional Proterozoic age.

*Acknowledgements* – This paper is the direct result of the geological work carried out by the author in connection with A/S Sydvaranger's prospecting activities in the Karasjok area. The analytical work was performed by M. Tysseland and S. Trovik at the University of Bergen, Norway. I am greatly indebted to the A/S Sydvaranger/Union Minerals joint venture for their permission to publish this paper, and to Dr. B. Robins for valuable comments and corrections of the English text.

REFERENCES

Arndt, N.T., Naldrett, A.J. & Pyke, D.R. 1977: Komatiitic and iron-rich tholeiitic lavas of Munro Township, Northeast Ontario. *J. Petrol. 18,* 319–369.

Arndt, N.T., Francis, C. & Hynes, A.J. 1979: The field characteristics and petrology of Archaean and Proterozoic komatiites. *Can. Mineral. 17,* 147–163.

Arndt, N.T. & Brooks, C. 1980: Komatiites: Penrose conference report. *Geology 8,* 155–156.

Arndt, N.T. & Nisbet, E.G. 1982: What is a komatiite? *In* Arndt, N.T. & Nisbet, E.G. (eds), *Komatiites.* Allen & Unwin Ltd., London 19–27.

Barbey, P., Convert, N.J., Martin, H., Mereau, B., Capdevila, R. & Hameur, J. 1980: Relationships between granite-gneiss terrains, greenstone belts and granulite belts in the Archaean crust of Lapland (Fennoscandia). *Geol. Rundschau 69,* 648–658.

Binns, R.A., Gunthorpe, R.J. & Groves, D.I. 1976: Metamorphic patterns and development of greenstone belts in the Eastern Yilgarn Block, Western Australia. *In* Windley, B.F. (ed.) *The early history of the earth,* John Wiley & Sons, Inc., New York.

Blais, S., Capdevila, R., Jahn, B.M., Bertrand, J.M. & Hameurt, J. 1978: The Archaean greenstone belts of Karelia (Eastern Finland) and their komatiitic and tholeiitic series. *In* Windley, B.F. & Naqvi, S.M. (eds.), *Archaean geochemistry.* Amsterdam: Elsevier, 87–107.

Bugge, J.A.W. 1960: Precambrian of Eastern Finnmark. *In:* O. Holtedahl (Ed.) Geology of Norway, *Norges geol. Unders. 208,* 78–92.

Bugge, J.A.W. 1980: The Sydvaranger type of quartz-banded iron ore, with a synopsis of Precambrian geology and ore deposits of Finnmark. *Geol. Surv. Finl. Bull. 307,* 17–24.

Condie, K.C. 1981: *Archaean Greenstone Belts.* (ed.) B.F. Windley. Developments in Precambrian Geology 3, Elsevier. Amsterdam.

Donaldson, C.H. 1974: Olivine crystal types in harrisitic rocks of the Rhum pluton and in Archaean spinifex rocks. *Geol. Soc. Am. Bull. 85,* 1727–1726.

Evans, B.W. & Trommsdorff, V. 1970: Regional metamorphism of ultramafic rocks in the central Alps-parageneses in the system $CaO$–$MgO$–$SiO_2$–$H_2O$. *Schweiz. Mineral. Petrog. Mitt. 50,* 481–492.

Evans, B.W. & Frost, B.R. 1975: Chrome-spinel in progressive metamorphism – a preliminary analysis. *Geochim. Cosmochim Acta 39,* 959–9—.

Frey, F.A., Bryan, W.B. & Thompson, 1974: Atlantic ocean floor geochemistry and petrology of basalts from legs 2 and 3 of the deep-sea drilling project. *J. Geophys. Res. 79,* 5505–5527.

Gaal, G., Mikkola, A. & Søderholm, B. 1978: Evolution of the Archaean crust in Finland. *Precamb. Res. 6,* 199–215.

Henriksen, H. 1980: Geological mapping in the area Karasjok–Skoganvarre. Unpubl. *A/S Sydvaranger archive report 1122,* 15 pp.

Henriksen, H. 1982: Geological mapping in the Karasjok area, 1982: Unpubl. *A/S Sydvaranger archive report 1232,* 33 pp.

Hyndman, D.W. 1972: *Petrology of igneous and metamorphic rocks.* McGraw Hill Book Company, New York.

Hörmann, P.K., Raith M., Raase P., Ackermand D. & Seifert F. 1980: The granulite complex of Finnish Lapland: Petrology and metamorphic conditions in the Ivalojoki–Inarijärvi area. *Geol. Surv. Finl. Bull. 3,* 95 pp.

Irvine, T.N., & Baragar, W.R.A. 1971: A guide to the chemical classification of the common volcanic rocks. *Can. J. Earth Sci. 8,* 523–548.

Jahn, B.M., Auvray, B., Blais, S., Capdevila, R., Cornichet, J., Vidal, F. & Haneurt, J. 1980: Trace-element geochemistry and petrogenesis of Finnish greenstone belts. *J. Petrol. 21,* 201–244.

Marston, R.J., Groves, D.I., Hudson, D.I. & Ross, J.R. 1981: Nickel sulfide deposits in Western Australia: A review. *Econ. Geol. 76,* 1330–1363.

Merilainen, K. 1976: The granulite complex and adjacent rocks in Lapland, northern Finland. *Geol. Surv. Finl. Bull. 281,* 1–129.

McQueen, K.G. 1981: Volcanic-associated nickel deposits from around the Widgiemooltha Dome, Western Australia. *Econ.Geol. 76,* 141 –1443.

Naldrett, A.J. & Goodwin, A.M. 1977: Volcanic rocks of the Blake River Group, Abititi greenstone belt, Ontario, and their sulphur content. *Can. J. Earth Sci. 14,* 539–550.

Naldrett, A.J. & Turner, A.B. 1977: The geology and petrogenesis of a greenstone belt and related nickel sulphide mineralization at Yakabindie, Western Australia. *Precamb. Res. 5,* 43–103.

Nesbitt, R.W. & Sun, S.S. 1976: Geochemistry of Archaean spinifex-textured peridotites and low-magnesian tholeiites. *Earth planet. Sci. Lett. 31,* 433–453.

Nesbitt, R.W. & Sun, S.S. 1980: Geochemical features of some Archaean and post-Archaean high-magnesian-low-alkali liquids. *Phil. Trans. R. Soc. London A 297,* 365–381.

Nesbitt, R.W., Sun, S.S. & Purvis, A.C. 1979: Komatiites: Geochemistry and genesis. *Canad. Miner. 17,* 165–186.

Nisbet, E.G., Bickle, M.J. & Martin, A. 1977: The mafic and ultramafic lavas of the Belingwe greenstone belt, Rhodesia. *J. Petrol. 18,* 521–566.

Nisbet, E.G. & Chinner, G.A, 1981: Controls of the eruption of mafic and ultramafic lavas, Ruth Well Ni-Cu prospect, West Pilbara *Econ.Geol. 76,* 1729–1735.

Pearce, T.H. 1968: A contribution to the theory of variation diagrams. *Contr. Mineral. Petrol. 19,* 142–157.

Pearce, T.H. 1969: Some comments on the differentiation of the Dundonald sill, Ontario. *Can. Jour. Earth. Sci. 6,* 75–80.

Pearce, J.A. & Norry, M.J. 1979: Petrogenetic implications of Ti, Zr, Y and Nb variations in volcanic rocks. *Contr. Miner. Petrol. 69,* 33–47.

Simonen, A. 1980: The Precambrian in Finland. *Geol. Surv. Finl. Bull. 30,* 58 pp.

Skålvoll, H. 1972: Beskrivelse til geologisk kart over Norge, 1:250 000 Karasjok. *Norges geol. Unders.*

Stolz, G.W. & Nesbitt, R.W. 1981: The komatiite nickel sulfide association at Scotia: A petrochemical investigation of the ore environment. Econ. Geol. 76, 1480–1502.

Viljoen, M.J. & Viljoen, R.P. 1969: The geology and geochemistry of the lower ultramafic unit of the Onverwacht Group and a proposed new class of igneous rock. *Spec. Publ. Geol. Soc. S. Afr. 2,* 55–85.

Vuagnat, M. 1975: Pillow lava flows, isolated sacks or connected tubes. *Bull. Volcanol. 39,* 1–9.

Wennervirta, H. 1969: Karasjokområdets geologi. *Norges geol. Unders. 252,* 132–183.

Winkler, H.G.F. 1976: *Petrogenesis of metamorphic rocks,* 4th. ed. 334 pp. Springer–Verlag, New York, Heidelberg, Berlin.

Willet, G., Eshuys, E. & Guy, B. 1978: Ultramafic rocks of the Widgemooltha-Norseman area, Western Australia: Petrological diversity, geochemistry and mineralization. *Precamb. Res. 6,* 133–156.